

# Parton-hadron dynamics in heavy-ion collisions

E. L. Bratkovskaya<sup>1,2</sup>, V. Ozvenchuk<sup>2,3</sup>, W. Cassing<sup>4</sup>, V. P. Konchakovski<sup>4</sup>, O. Linnyk<sup>4</sup>, R. Marty<sup>1,2</sup>, and H. Berrehrh<sup>1,2</sup>

<sup>1</sup> *Institute for Theoretical Physics, University of Frankfurt, Frankfurt, Germany*

<sup>2</sup> *Frankfurt Institute for Advanced Study, Frankfurt am Main, Germany*

<sup>3</sup> *SUBATECH, UMR 6457, Laboratoire de Physique Subatomique et des Technologies Associées, University of Nantes - IN2P3/CNRS - Ecole des Mines de Nantes, Nantes Cedex 03, France and*

<sup>4</sup> *Institute for Theoretical Physics, University of Giessen, Giessen, Germany*

(Dated: September 25, 2021)

The dynamics of partons and hadrons in relativistic nucleus-nucleus collisions is analyzed within the novel Parton-Hadron-String Dynamics (PHSD) transport approach, which is based on a dynamical quasiparticle model for the partonic phase (DQPM) including a dynamical hadronization scheme. The PHSD approach is applied to nucleus-nucleus collisions from low SPS to LHC energies. The traces of partonic interactions are found in particular in the elliptic flow of hadrons and in their transverse mass spectra. We investigate also the equilibrium properties of strongly-interacting infinite parton-hadron matter characterized by transport coefficients such as shear and bulk viscosities and the electric conductivity in comparison to lattice QCD results.

PACS numbers:

## I. INTRODUCTION

According to present understanding our universe has been created in a 'Big Bang' about  $1,37 \cdot 10^{10}$  years ago. The 'Big Bang' scenario implies that in the first micro-seconds of the universe the entire state has emerged from a partonic system of quarks, antiquarks and gluons – a quark-gluon plasma (QGP) – to color neutral hadronic matter consisting of interacting hadronic states (and resonances) in which the partonic degrees of freedom are confined. The nature of confinement and the dynamics of this phase transition has motivated a large community for several decades and is still an outstanding question of today's physics. Early concepts of the QGP were guided by the idea of a weakly interacting system of partons which might be described by perturbative QCD (pQCD). However, experimental observations at the Relativistic Heavy Ion Collider (RHIC) indicated that the new medium created in ultrarelativistic Au+Au collisions is interacting more strongly than hadronic matter and consequently this concept had to be severely questioned. Moreover, in line with theoretical studies in Refs. [1–3] the medium showed phenomena of an almost perfect liquid of partons [4, 5] as extracted from the strong radial expansion and the scaling of elliptic flow  $v_2(p_T)$  of mesons and baryons with the number of constituent quarks and antiquarks [4]. Indeed, recent relativistic viscous hydrodynamic calculations - using the Israel-Stewart framework - require a very small shear viscosity to entropy density ratio  $\eta/s$  of  $0.08 - 0.24$  in order to reproduce the elliptic flow  $v_2$  data at RHIC (cf. [6]). There is strong evidence from atomic and molecular systems that  $\eta/s$  should have a minimum in the vicinity of the phase transition (or rapid crossover) between the hadronic matter and the quark-gluon plasma [7], and that the ratio of bulk viscosity to entropy density  $\zeta/s$  should be maximum or even diverge at a second-order phase transition [8]. It is also important to know the electromagnetic properties of the QGP, such as the electric conductivity, since it determines the electromagnetic radiation in terms of photons and dileptons.

The question about the properties of this (nonperturbative)

QGP 'liquid' is discussed controversially in the literature and dynamical concepts describing the formation of color neutral hadrons from colored partons are scarce. A fundamental issue for hadronization models is the conservation of 4-momentum as well as the entropy problem, because by fusion/coalescence of massless (or low constituent mass) partons to color neutral bound states of low invariant mass (e.g. pions) the number of degrees of freedom and thus the total entropy is reduced in the hadronization process. This problem - a violation of the second law of thermodynamics as well as the conservation of four-momentum and flavor currents - has been addressed in Ref. [9] on the basis of the DQPM employing covariant transition rates for the fusion of 'massive' quarks and antiquarks to color neutral hadronic resonances or strings. In fact, the dynamical studies for an expanding partonic fireball in Ref. [9] suggest that these problems have come to a practical solution.

A consistent dynamical approach - valid also for strongly interacting systems - can be formulated on the basis of Kadanoff-Baym (KB) equations [10] or off-shell transport equations in phase-space representation, respectively [10]. In the KB theory the field quanta are described in terms of dressed propagators with complex selfenergies. Whereas the real part of the selfenergies can be related to mean-field potentials (of Lorentz scalar, vector or tensor type), the imaginary parts provide information about the lifetime and/or reaction rates of time-like 'particles' [11]. Once the proper (complex) selfenergies of the degrees of freedom are known the time evolution of the system is fully governed by off-shell transport equations (as described in Refs. [10, 11]). The determination/extraction of complex selfenergies for the partonic degrees of freedom has been performed before in Ref. [12] by fitting lattice QCD (lQCD) 'data' within the Dynamical QuasiParticle Model (DQPM). In fact, the DQPM allows for a simple and transparent interpretation of lattice QCD results for thermodynamic quantities as well as correlators and leads to effective strongly interacting partonic quasiparticles with broad spectral functions. For a review on off-shell transport theory and results from the DQPM in comparison to lQCD

we refer the reader to Ref. [11].

The actual implementations in the PHSD transport approach have been presented in detail in Refs. [13, 14]. Here we present results for transverse mass spectra and elliptic flow of hadrons for heavy-ion collisions at relativistic energies in comparison to data from the experimental collaborations.

## II. THE PHSD APPROACH

The dynamics of partons, hadrons and strings in relativistic nucleus-nucleus collisions is analyzed here within the Parton-Hadron-String Dynamics approach [9, 13, 14]. In this transport approach the partonic dynamics is based on Kadanoff-Baym equations for Green functions with self-energies from the Dynamical QuasiParticle Model (DQPM) [12] which describes QCD properties in terms of 'resummed' single-particle Green functions. In Ref. [14], the actual three DQPM parameters for the temperature-dependent effective coupling were fitted to the recent lattice QCD results of Ref. [16]. The latter lead to a critical temperature  $T_c \approx 160$  MeV which corresponds to a critical energy density of  $\epsilon_c \approx 0.5$  GeV/fm<sup>3</sup>. In PHSD the parton spectral functions  $\rho_j$  ( $j = q, \bar{q}, g$ ) are no longer  $\delta$ -functions in the invariant mass squared as in conventional cascade or transport models but depend on the parton mass and width parameters:

$$\rho_j(\omega, \mathbf{p}) = \frac{\gamma_j}{E_j} \left( \frac{1}{(\omega - E_j)^2 + \gamma_j^2} - \frac{1}{(\omega + E_j)^2 + \gamma_j^2} \right) \quad (1)$$

separately for quarks/antiquarks and gluons ( $j = q, \bar{q}, g$ ). With the convention  $E^2(\mathbf{p}^2) = \mathbf{p}^2 + M_j^2 - \gamma_j^2$ , the parameters  $M_j^2$  and  $\gamma_j$  are directly related to the real and imaginary parts of the retarded self-energy, *e.g.*  $\Pi_j = M_j^2 - 2i\gamma_j\omega$ . The spectral function (1) is antisymmetric in  $\omega$  and normalized as

$$\int_{-\infty}^{\infty} \frac{d\omega}{2\pi} \omega \rho_j(\omega, \mathbf{p}) = \int_0^{\infty} \frac{d\omega}{2\pi} 2\omega \rho_j(\omega, \mathbf{p}) = 1. \quad (2)$$

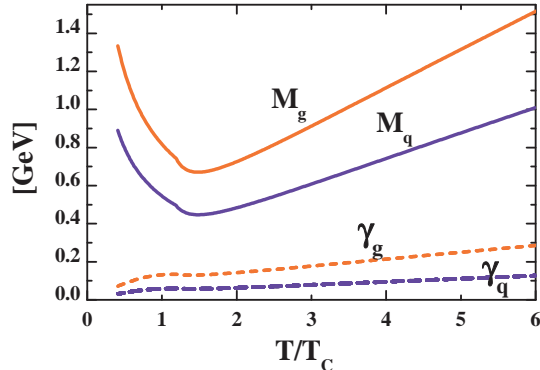


FIG. 1: The effective gluon mass  $M_g$  and width  $\gamma_g$  as function of the scaled temperature  $T/T_c$  (red lines). The blue lines show the corresponding quantities for quarks.

The actual parameters in Eq. (1), *i.e.* the gluon mass  $M_g$  and width  $\gamma_g$  – employed as input in the PHSD calculations

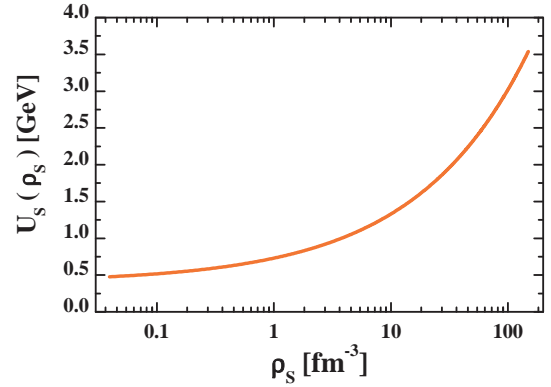


FIG. 2: The scalar mean field (3) for quarks and antiquarks from the DQPM as a function of the scalar parton density  $\rho_s$  (2).

– as well as the quark mass  $M_q$  and width  $\gamma_q$ , are depicted in Fig. 1 as a function of the scaled temperature  $T/T_c$ . As mentioned above these values for the masses and widths have been fixed by fitting the lattice QCD results from Ref. [16] in thermodynamic equilibrium.

A scalar mean-field  $U_s(\rho_s)$  for quarks and antiquarks can be defined by the derivative,

$$U_s(\rho_s) = \frac{dV_p(\rho_s)}{d\rho_s}, \quad (3)$$

which is evaluated numerically within the DQPM. Here  $V_p$  is a potential energy density

$$V_p(T, \mu_q) = T_g^{00}(T, \mu_q) + T_q^{00}(T, \mu_q) + T_{\bar{q}}^{00}(T, \mu_q) \quad (4)$$

where the different contributions  $T_j^{00}$  correspond to the space-like part of the energy-momentum tensor component  $T_j^{00}$  of parton  $j = g, q, \bar{q}$  (cf. Section 3 in Ref. [12]). The scalar mean-field  $U_s(\rho_s)$  for quarks and antiquarks is displayed in Fig. 2 as a function of the parton scalar density  $\rho_s$  and shows that the scalar mean field is in the order of a few GeV for  $\rho_s > 10$  fm<sup>-3</sup>. The mean-field (3) is employed in the PHSD transport calculations and determines the force on a quasiparticle  $j$ , *i.e.*  $\sim M_j/E_j \nabla U_s(x) = M_j/E_j dU_s/d\rho_s \nabla \rho_s(x)$  where the scalar density  $\rho_s(x)$  is determined numerically on a space-time grid.

Furthermore, a two-body interaction strength can be extracted from the DQPM as well from the quasiparticle width in line with Ref. [3]. The transition from partonic to hadronic d.o.f. (and vice versa) is described by covariant transition rates for the fusion of quark-antiquark pairs or three quarks (antiquarks), respectively, obeying flavor current-conservation, color neutrality as well as energy-momentum conservation [13, 14]. Since the dynamical quarks and antiquarks become very massive close to the phase transition, the formed resonant prehadronic color-dipole states ( $q\bar{q}$  or  $qqq$ ) are of high invariant mass, too, and sequentially decay to the groundstate meson and baryon octets increasing the total entropy.

On the hadronic side PHSD includes explicitly the baryon octet and decouplet, the  $0^-$ - and  $1^-$ -meson nonets as well as

selected higher resonances as in the Hadron-String-Dynamics (HSD) approach [17–19]. The color-neutral objects of higher masses ( $>1.5$  GeV in case of baryonic states and  $>1.3$  GeV in case of mesonic states) are treated as ‘strings’ (color-dipoles) that decay to the known (low-mass) hadrons according to the JETSET algorithm [20]. We discard an explicit recapitulation of the string formation and decay and refer the reader to the original work [20]. Note that PHSD and HSD (without explicit partonic degrees-of-freedom) merge at low energy density, in particular below the critical energy density  $\varepsilon_c \approx 0.5$  GeV/fm<sup>3</sup>.

### III. APPLICATION TO NUCLEUS-NUCLEUS COLLISIONS

The PHSD approach was applied to nucleus-nucleus collisions from  $s_{NN}^{1/2} \sim 5$  to 200 GeV in Refs. [13–15] in order to explore the space-time regions of partonic matter. It was found that even central collisions at the top-SPS energy of  $\sqrt{s_{NN}} = 17.3$  GeV show a large fraction of nonpartonic, *i.e.* hadronic or string-like matter, which can be viewed as a hadronic corona [21]. This finding implies that neither hadronic nor only partonic models can be employed to extract physical conclusions in comparing model results with data.

#### A. Transverse mass spectra

It is of interest, how the PHSD approach compares to the HSD [18] model (without explicit partonic degrees-of-freedom) as well as to experimental data. In Fig. 3 we show the transverse mass spectra of  $\pi^-$ ,  $K^+$  and  $K^-$  mesons for 7% central Pb+Pb collisions at 40 and 80 A·GeV and 5% central collisions at 158 A·GeV in comparison to the data of the NA49 Collaboration [22]. Here the slope of the  $\pi^-$  spectra is only slightly enhanced in PHSD relative to HSD which demonstrates that the pion transverse motion shows no sizeable sensitivity to the partonic phase. However, the  $K^\pm$  transverse mass spectra are substantially hardened with respect to the HSD calculations at all bombarding energies - *i.e.* PHSD is more in line with the data - and thus suggests that partonic effects are better visible in the strangeness-degrees of freedom.

The PHSD calculations for RHIC energies show a very similar trend - the inverse slope increases by including the partonic phase - cf. Fig. 4 where we show the transverse mass spectra of  $\pi^-$ ,  $K^+$  and  $K^-$  mesons for 5% central Au+Au collisions at  $\sqrt{s} = 200$  GeV in comparison to the data of the RHIC Collaborations [23–25].

The hardening of the kaon spectra can be traced back to parton-parton scattering as well as a larger collective acceleration of the partons in the transverse direction due to the presence of repulsive vector fields for the partons. The enhancement of the spectral slope for kaons and antikaons in PHSD due to collective partonic flow shows up much clearer for the kaons due to their significantly larger mass (relative to pions). We recall that in Refs. [26] the underestimation of the

$K^\pm$  slope by HSD (and also UrQMD) had been suggested to be a signature for missing partonic degrees of freedom; the present PHSD calculations support this early suggestion.

The strange antibaryon sector is of further interest since here the HSD calculations have always underestimated the yield [27]. Our detailed studies in Ref. [13] show that the HSD and PHSD calculations both give a reasonable description of the  $\Lambda + \Sigma^0$  yield of the NA49 Collaboration [28]; both models underestimate the NA57 data [29] by about 30%. An even larger discrepancy in the data from the NA49 and NA57 Collaborations is seen for  $(\bar{\Lambda} + \bar{\Sigma}^0)/N_{wound}$ ; here the PHSD calculations give results which are in between the NA49 data and the NA57 data whereas HSD underestimates the  $(\bar{\Lambda} + \bar{\Sigma}^0)$  midrapidity yield at all centralities.

The latter result suggests that the partonic phase does not show up explicitly in an enhanced production of strangeness (or in particular strange mesons and baryons) but leads to a different redistribution of anti-strange quarks between mesons and antibaryons. In fact, as demonstrated in Ref. [13], we find no sizeable differences in the double strange baryons from HSD and PHSD – in a good agreement with the NA49 data – but observe a large enhancement in the double strange antibaryons for PHSD relative to HSD.

#### B. Collective flow

The anisotropy in the azimuthal angle  $\psi$  is usually characterized by the even order Fourier coefficients  $v_n = \langle \exp(in(\psi - \Psi_{RP})) \rangle$ ,  $n = 2, 4, \dots$ , since for a smooth angular profile the odd harmonics become equal to zero. As noted above,  $\Psi_{RP}$  is the azimuth of the reaction plane and the brackets denote averaging over particles and events. In particular, for the widely used second order coefficient, denoted as an elliptic flow, we have

$$v_2 = \langle \cos(2\psi - 2\Psi_{RP}) \rangle = \left\langle \frac{p_x^2 - p_y^2}{p_x^2 + p_y^2} \right\rangle, \quad (5)$$

where  $p_x$  and  $p_y$  are the  $x$  and  $y$  components of the particle momenta. This coefficient can be considered as a function of centrality, pseudo-rapidity  $\eta$  and/or transverse momentum  $p_T$ . We note that the reaction plane in PHSD is given by the  $(x - z)$  plane with the  $z$ -axis in the beam direction.

In Fig. 5 the experimental  $v_2$  excitation function in the transient energy range is compared to the results from the PHSD calculations [35]; HSD model results are given as well for reference. We note that the centrality selection and acceptance are the same for the data and models.

We recall that the HSD model has been very successful in describing heavy-ion spectra and rapidity distributions from SIS to SPS energies. A detailed comparison of HSD results with respect to a large experimental data set was reported in Refs. [26, 32, 33] for central Au+Au (Pb+Pb) collisions from SIS to top SPS energies. Indeed, as shown in Fig. 5 (dashed lines), HSD is in good agreement with experiment for both data sets at the lower edge ( $\sqrt{s_{NN}} \sim 10$  GeV) but predicts an approximately energy-independent flow  $v_2$  at larger energies

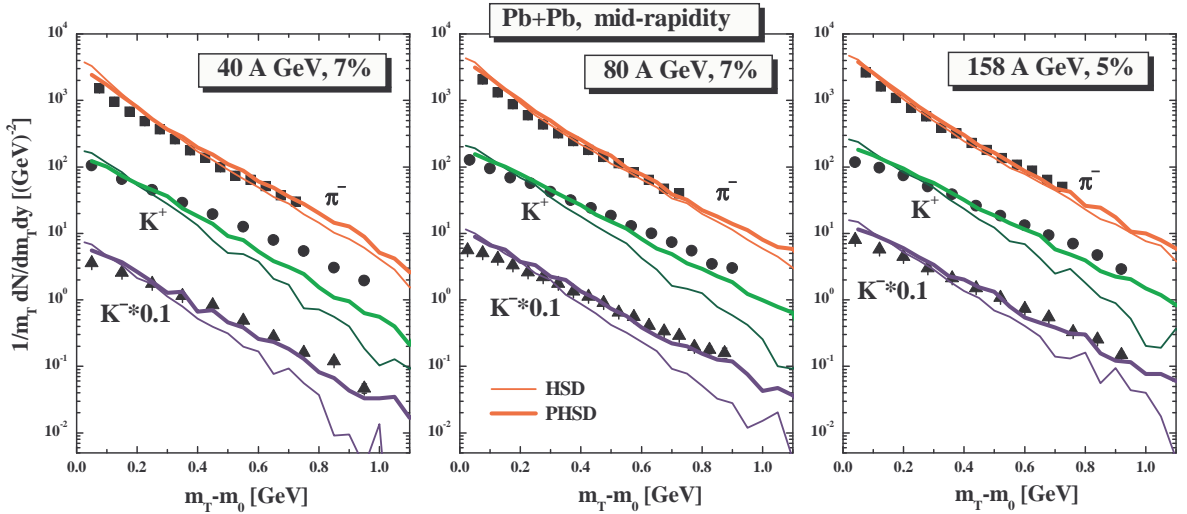


FIG. 3: The  $\pi^-$ ,  $K^+$  and  $K^-$  transverse mass spectra for central Pb+Pb collisions at 40, 80 and 158 A-GeV from PHSD (thick solid lines) in comparison to the distributions from HSD (thin solid lines) and the experimental data from the NA49 Collaboration [22].

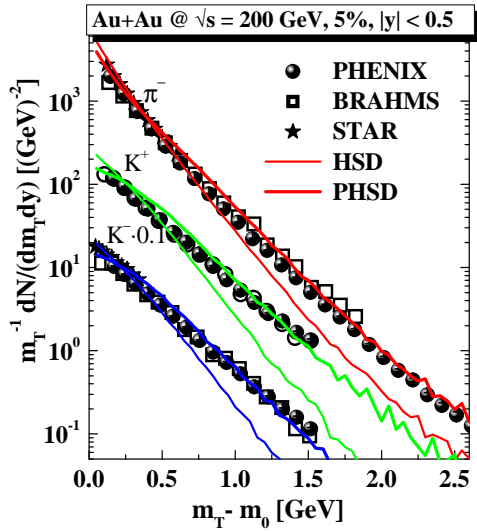


FIG. 4: The  $\pi^-$ ,  $K^+$  and  $K^-$  transverse mass spectra for 5% central Au+Au collisions at  $\sqrt{s} = 200$  GeV from PHSD (thick solid lines) in comparison to the distributions from HSD (thin solid lines) and the experimental data from the BRAHMS, PHENIX and STAR Collaborations [23–25] at midrapidity.

and, therefore, does not match the experimental observations. This behavior is in quite close agreement with another independent hadronic model, the UrQMD (Ultra relativistic Quantum Molecular Dynamics) [34] (cf. with Ref. [30]).

From the above comparison one may conclude that the rise of  $v_2$  with bombarding energy is not due to hadronic interactions and models with partonic d.o.f. have to be addressed. Indeed, the PHSD approach incorporates the parton medium effects in line with a IQCD equation-of-state, as discussed above, and also includes a dynamic hadronization scheme

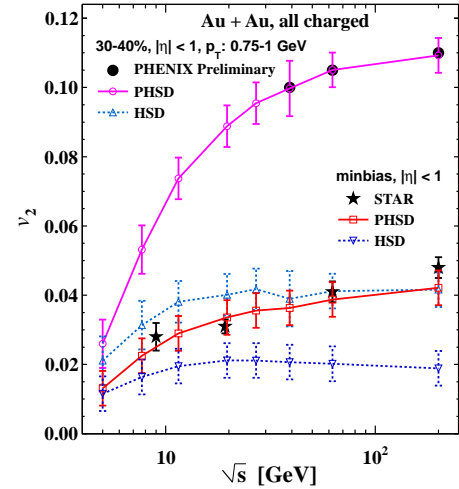


FIG. 5: Average elliptic flow  $v_2$  of charged particles at midrapidity for two centrality selections calculated within the PHSD (solid curves) and HSD (dashed curves). The  $v_2$  STAR data compilation for minimal bias collisions are taken from [30] (stars) and the preliminary PHENIX data [31] are plotted by filled circles.

based on covariant transition rates. It is seen from Fig. 5 that PHSD performs better: The elliptic flow  $v_2$  from PHSD (solid curve) is fairly in line with the data from the STAR and PHENIX collaborations and clearly shows the growth of  $v_2$  with the bombarding energy [35].

The  $v_2$  increase is clarified in Fig. 6 where the partonic fraction of the energy density at mid-pseudorapidity with respect to the total energy density in the same pseudorapidity interval is shown. We recall that the repulsive mean-field potential  $U(\rho_v)$  for partons in the PHSD model leads to an increase of the flow  $v_2$  as compared to that for HSD or PHSD calculations without partonic mean fields. As follows from Fig. 6,

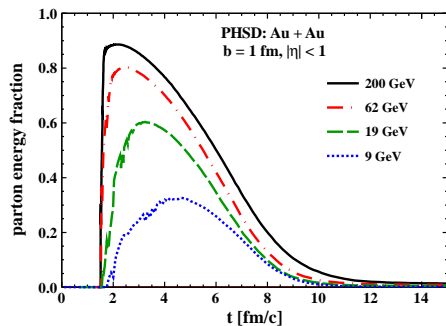


FIG. 6: The evolution of the parton fraction of the total energy density at mid-pseudorapidity for different collision energies.

the energy fraction of the partons substantially grows with increasing bombarding energy while the duration of the partonic phase is roughly the same.

#### IV. TRANSPORT COEFFICIENTS

In this Section we concentrate on the extraction of equilibrium properties of ‘infinite’ parton-hadron matter characterized by transport coefficients such as shear and bulk viscosity and electric conductivity which have been studied within the PHSD approach in Refs. [43–45].

We simulate the ‘infinite’ matter within a cubic box with periodic boundary conditions at various values for the quark density (or chemical potential) and energy density. The size of the box is fixed to  $9^3 \text{ fm}^3$ . The initialization is done by populating the box with light ( $u, d$ ) and strange ( $s$ ) quarks, antiquarks and gluons. The system is initialized out of equilibrium and approaches kinetic and chemical equilibrium during its evolution by PHSD. If the energy density in the system is below the critical energy density ( $\varepsilon_c \approx 0.5 \text{ GeV}/\text{fm}^3$ ), the evolution proceeds through the dynamical phase transition (as described in Ref. [43]) and ends up in an ensemble of interacting hadrons. The transport properties are calculated employing the Kubo formalism [38, 39] and relaxation time approximation [40–42]. For more details we refer the reader to Ref. [43].

In Fig. 7 we present the PHSD results for the shear and bulk viscosities of partonic and hadronic matter - as well as the electric conductivity - as a function of the temperature  $T/T_c$  ( $T_c = 158 \text{ MeV}$ ). The ratio of the shear viscosity to entropy density  $\eta(T)/s(T)$  from PHSD shows a minimum

(with a value of about 0.1) close to the critical temperature  $T_c$ , while it approaches the perturbative QCD (pQCD) limit at higher temperatures in line with lattice QCD results. For  $T < T_c$ , i.e. in the hadronic phase, the ratio  $\eta/s$  rises fast with decreasing temperature due to a lower interaction rate of the hadronic system and a significantly smaller number of degrees-of-freedom.

The bulk viscosity  $\zeta(T)$  – evaluated in the relaxation time approach – is found to strongly depend on the effects of mean fields (or potentials) in the partonic phase. We find a significant rise of the ratio  $\zeta(T)/s(T)$  in the vicinity of the critical temperature  $T_c$ , which is also in agreement with that from IQCD calculations. This rise has to be attributed to mean-fields (or potential) effects that in PHSD are encoded in the temperature dependence of the quasiparticle masses, which is related to the infrared enhancement of the resummed (effective) coupling  $g(T)$ .

We also find that the dimensionless ratio of the electric conductivity over temperature  $\sigma_0/T$  rises above  $T_c$  approximately linearly with  $T$  up to  $T = 2.5T_c$ , but approaches a constant above  $5T_c$ , as expected qualitatively from perturbative QCD (pQCD) (cf. Ref. [45] for details). Our findings imply that the QCD matter even at  $T \approx T_c$  is a much better electric conductor than  $Cu$  or  $Ag$  (at room temperature). We note that our result for  $\sigma_0/T$  close to  $T_c$  is in agreement with the most recent IQCD calculations which is important for the photon emission rate from the QGP or the hadronic system which is controlled by the electric conductivity.

#### V. SUMMARY

Since the PHSD calculations have proven to describe single-particle as well as collective observables from relativistic nucleus-nucleus collisions from lower SPS to top RHIC energies [15], the extracted transport coefficients  $\eta(T)$ ,  $\zeta(T)$  and  $\sigma_0(T)$  are compatible with experimental observations in a wide energy density (temperature) range. Furthermore, the qualitative and partly quantitative agreement with IQCD transport coefficients is striking and should be further explored in future.

#### Acknowledgments

This work in part has been supported by the LOEWE center HIC for FAIR as well as DFG.

[1] Shuryak, E.: 2004, Prog. Part. Nucl. Phys. 53, 273  
 [2] Thoma, M. H.: 2005, J. Phys. G 31, L7; 2006, Nucl. Phys. A 774, 307  
 [3] Peshier, A. and Cassing, W.: 2005, Phys. Rev. Lett. 94, 172301  
 [4] Arsene, I. *et al.*: 2005, Nucl. Phys. A 757, 1; Back, B. B. *et al.*: 2005, Nucl. Phys. A 757, 28; Adams, J. *et al.*: 2005, Nucl. Phys. A 757, 102; Adcox, K. *et al.*: 2005, Nucl. Phys. A 757,

184  
 [5] Hirano, T. and Gyulassy, M.: 2006, Nucl. Phys. A 769, 71  
 [6] Romatschke, P. and Romatschke, U.: 2007, Phys. Rev. Lett. 99, 172301  
 [7] Csernai, L. P., Kapusta, J. I. and McLerran, L. D.: 2006, Phys. Rev. Lett. 97, 152303  
 [8] Kharzeev, D. and Tuchin, K.: 2008, JHEP 09, 093

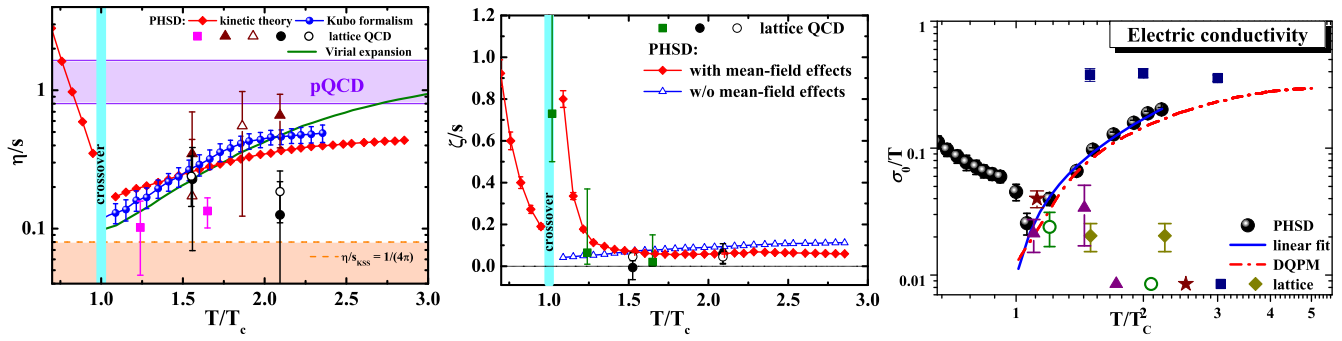


FIG. 7: The PHSD results for the shear (upper part) and bulk (middle part) viscosities of partonic and hadronic matter - as well as the electric conductivity (lower part) - as a function of the scaled temperature  $T/T_c$ .

- [9] Cassing, W. and Bratkovskaya, E. L.: 2008, Phys. Rev. C 78, 034919
- [10] Juchem, S., Cassing, W. and Greiner, C.: 2004, Phys. Rev. D 69, 025006; 2004, Nucl. Phys. A 743, 92
- [11] Cassing, W.: 2009, E. Phys. J. ST 168, 3
- [12] Cassing, W.: 2007, Nucl. Phys. A 795, 70; 2007, Nucl. Phys. A 791, 365
- [13] Cassing, W. and Bratkovskaya, E. L.: 2009, Nucl. Phys. A 831, 215
- [14] Bratkovskaya, E.L., Cassing, W., Konchakovski, V. P., and Linnyk, O.: 2011, Nucl. Phys. A 856, 162
- [15] Konchakovski, V. P. *et al.*: 2012, Phys. Rev. C 85, 044922
- [16] Aoki, Y. *et al.*: 2009, JHEP 0906, 088; Borsanyi, S., Endrodi, G., Fodor, Z. *et al.*: 2010, JHEP 1011, 077
- [17] Ehehalt, W. and Cassing, W.: 1996, Nucl. Phys. A 602, 449
- [18] Cassing, W. and Bratkovskaya, E. L.: 1999, Phys. Rep. 308, 65
- [19] Cassing, W.: 2002, Nucl. Phys. A 700, 618
- [20] Bengtsson, H.-U. and Sjöstrand, T.: 1987, Comp. Phys. Commun. 46, 43
- [21] Aichelin, J. and Werner, K.: 2009, Phys. Rev. C 79, 064907
- [22] Alt, C. *et al.*: 2002, Phys. Rev. C 66, 054902; 2008, Phys. Rev. C 77, 024903
- [23] Adler, S. S. *et al.*: 2004, Phys. Rev. C 69, 034909
- [24] Adams, J. *et al.*: 2004, Phys. Rev. Lett. 92, 112301
- [25] Bearden, I. G. *et al.*: 2005, Phys. Rev. Lett. 94, 162301
- [26] Bratkovskaya, E. L., Soff, S., Stöcker, H., van Leeuwen, M., and Cassing, W.: 2004, Phys. Rev. Lett. 92, 032302
- [27] Geiss, J., Cassing, W. and Greiner, C.: 1998, Nucl. Phys. A 644, 107
- [28] Anticic, T. *et al.*: 2009, Phys. Rev. C 80, 034906
- [29] Antinori, F. *et al.*: 2004, Phys. Lett. B 595, 68; 2006, J. Phys. G: Nucl. Phys. 32, 427
- [30] Nasim, M., Kumar, L., Netrakanti, P.K., and Mohanty, B.: 2010, Phys. Rev. C 82, 054908
- [31] Gong, X. *et al.*: 2011, J. Phys. G 38, 124146
- [32] Bratkovskaya, E. L., Cassing, W., and Mosel, U.: 1998, Phys. Lett. B 424, 244
- [33] Bratkovskaya, E. L. *et al.*: 2004, Phys. Rev. C 69, 054907
- [34] Bass, S. A. *et al.*: 1998, Prog. Part. Nucl. Phys. 41, 255; Bleicher, M. *et al.*: 1999, J. Phys. G 25, 1859
- [35] Konchakovski V. P. *et al.*: 2012, Phys. Rev. C 85, 011902(R)
- [36] Voloshin, S. A.: 2007, J. Phys. G 34, S883
- [37] Shimomura, M. *et al.*: 2011, PoS WPCF2011, 070
- [38] Green, M. S.: 1954, J. of Chem. Phys. 22, 398
- [39] Kubo, R.: 1957, J. Phys. Soc. Japan 12, 570; 1966, Rep. Prog. Phys. 29, 255
- [40] Hosoya, A. and Kajantie, K.: 1985, Nucl. Phys. B 250, 666
- [41] Gavin, S.: 1985, Nucl. Phys. A 435, 826
- [42] Chakraborty, P. and Kapusta, J. I.: 2011, Phys. Rev. C 83, 014906
- [43] Ozvenchuk, V. *et al.*: 2013, Phys. Rev. C 87, 024901
- [44] Marty, R., Bratkovskaya, E., Cassing, W., Aichelin, J. and Berrehrh, H.: 2013, Phys. Rev. C 88, 045204
- [45] Cassing, W., Linnyk, O., Steinert, T., Ozvenchuk, V.: 2013, Phys. Rev. Lett. 110, 182301